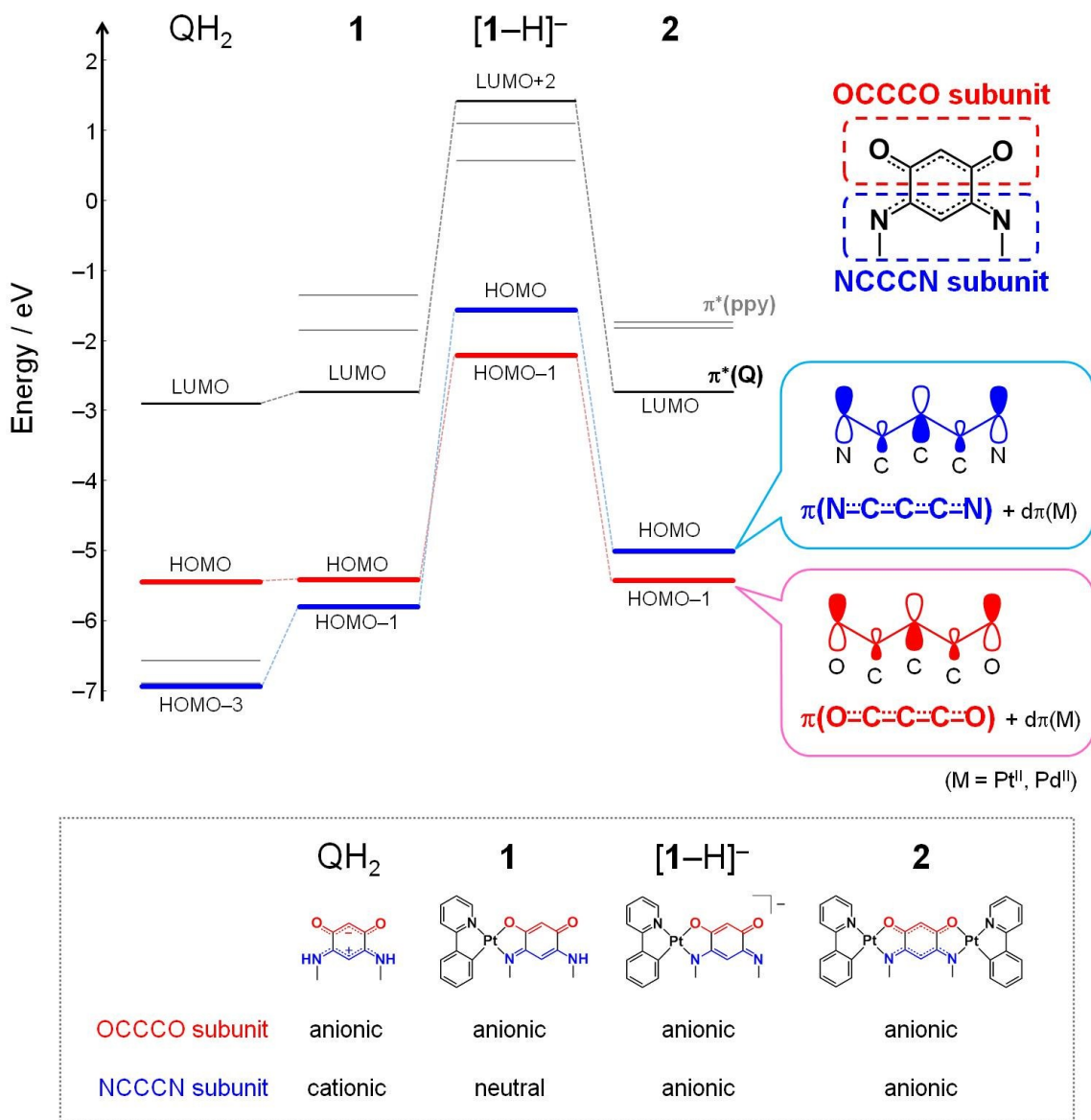


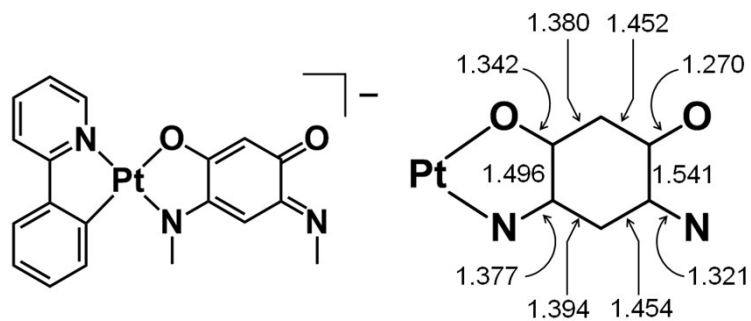
Supporting information

Colour tuning by the stepwise synthesis of mononuclear and homo- and hetero-dinuclear platinum(II) complexes using a zwitterionic quinonoid ligand

Paramita Kar, Masaki Yoshida, Atsushi Kobayashi, Lucie Routaboul, Pierre Braunstein, Masako Kato



Scheme S1. Molecular orbital diagrams of QH_2 , **1**, $[\text{1}-\text{H}]^-$ (= deprotonated form of **1**), and **2** calculated by the DFT method. Orbitals represented as blue and red lines are π orbitals involving NCCCN and OCCCO subunits, respectively (the detailed results of the DFT calculations for QH_2 and $[\text{1}-\text{H}]^-$ are shown in Fig. S8 and Scheme S2).



Scheme S2. Calculated bond distances in quinonoid ligand Q^{2-} in the optimized structure of $[\mathbf{1}-\text{H}]^-$. In contrast to the *p*-quinone like structure of **1**, ligand Q^{2-} of $[\mathbf{1}-\text{H}]^-$ adopted *o*-quinone form in this optimized structure, presumably due to the polarization by the positively charged Pt(II) center.

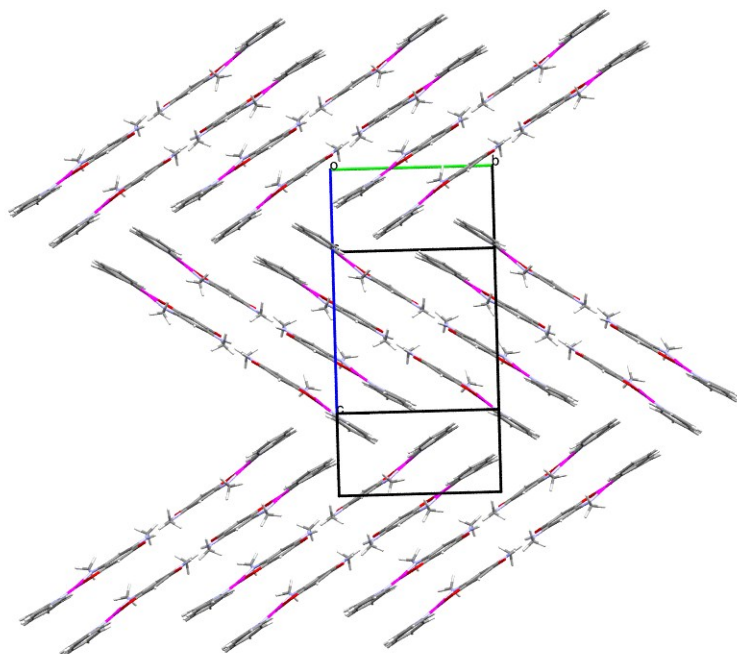


Fig. S1. Packing structure of complex **1**.

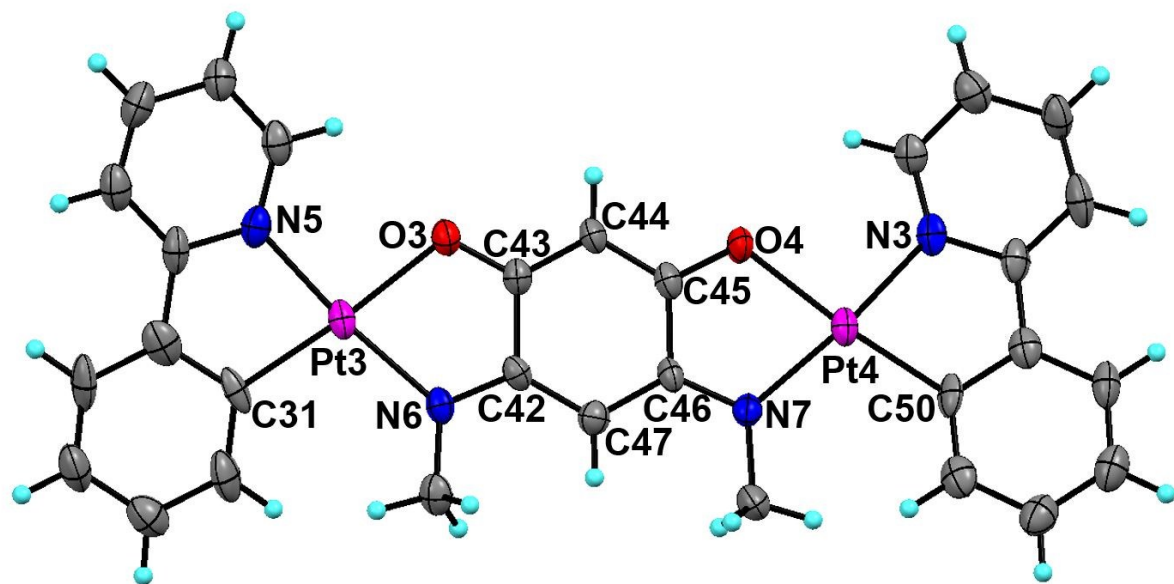


Fig. S2. Coordination environment around the metal centers in one crystallographically independent dinuclear unit complex **2**. Coordination environment of another unit is shown in main manuscript.

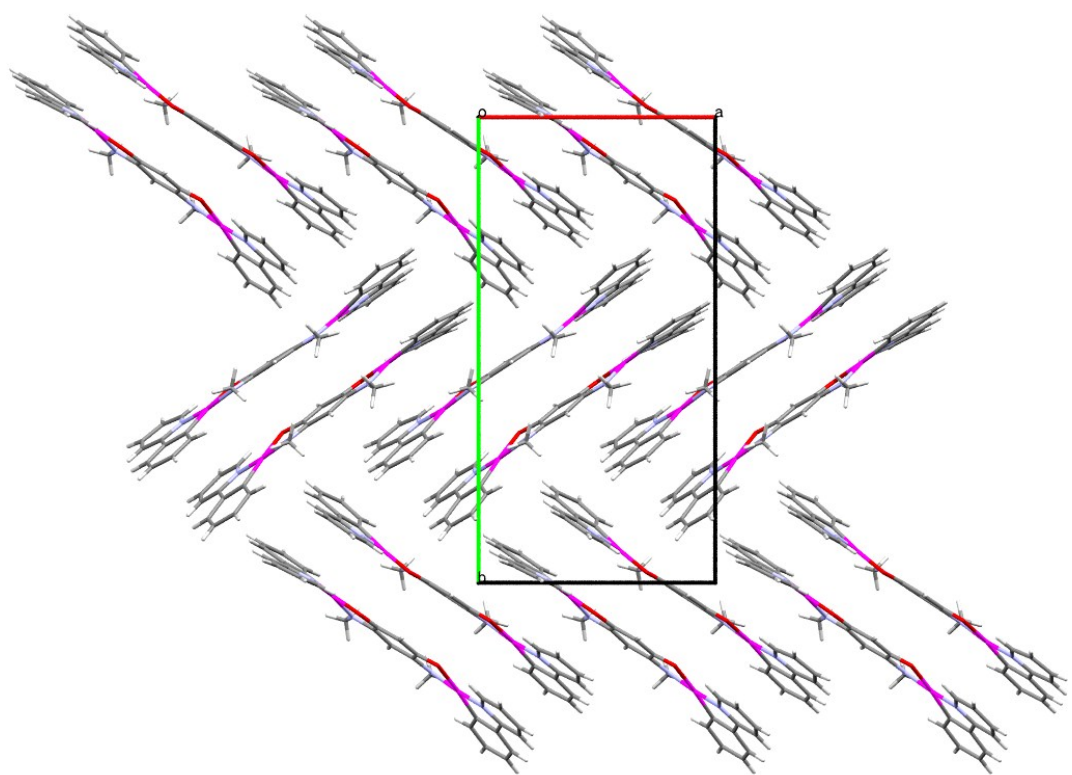


Fig. S3. Packing structure of complex **2**.

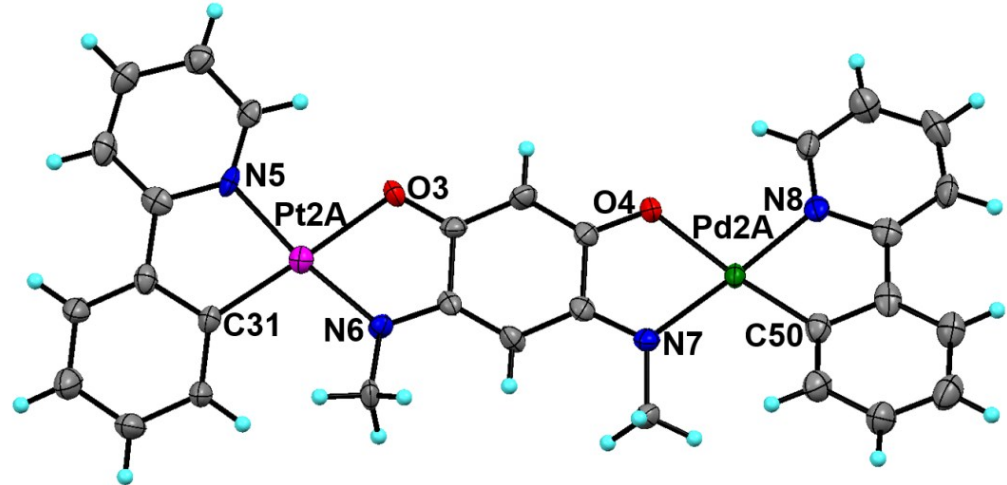


Fig. S4. Coordination environment around the metal centers in one crystallographically independent dinuclear unit complex **3**. Coordination environment of another unit is shown in main manuscript.

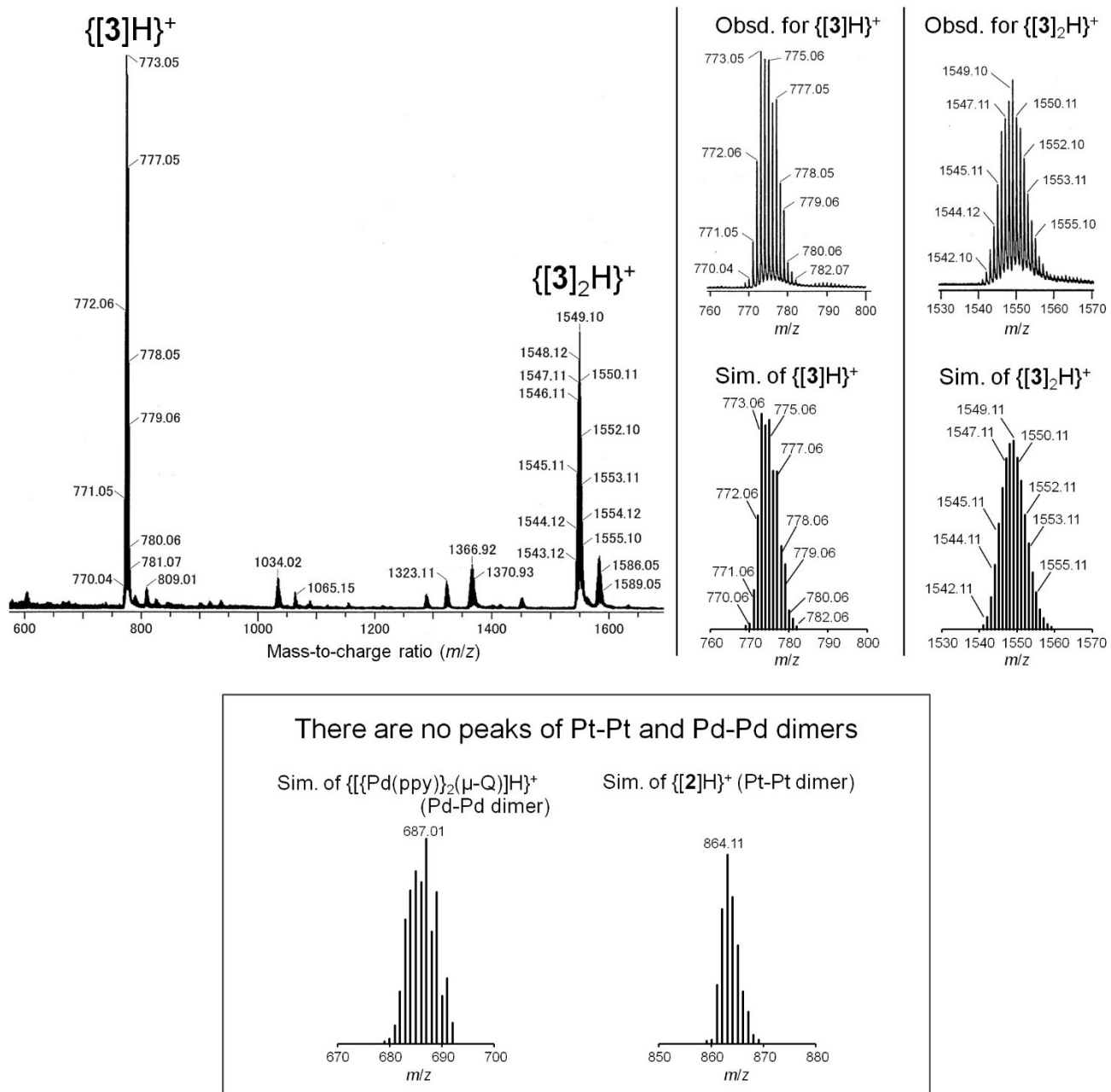


Fig. S5. ESI-TOF mass spectrum of **3** in CHCl_3 together with the simulation patterns of the molecular ions $[\mathbf{3} + \mathbf{H}]^+$ and $\{\mathbf{3}\}_2 + \mathbf{H}^+$. Note that there are no peaks of Pt-Pt and Pd-Pd dimers in the spectrum.

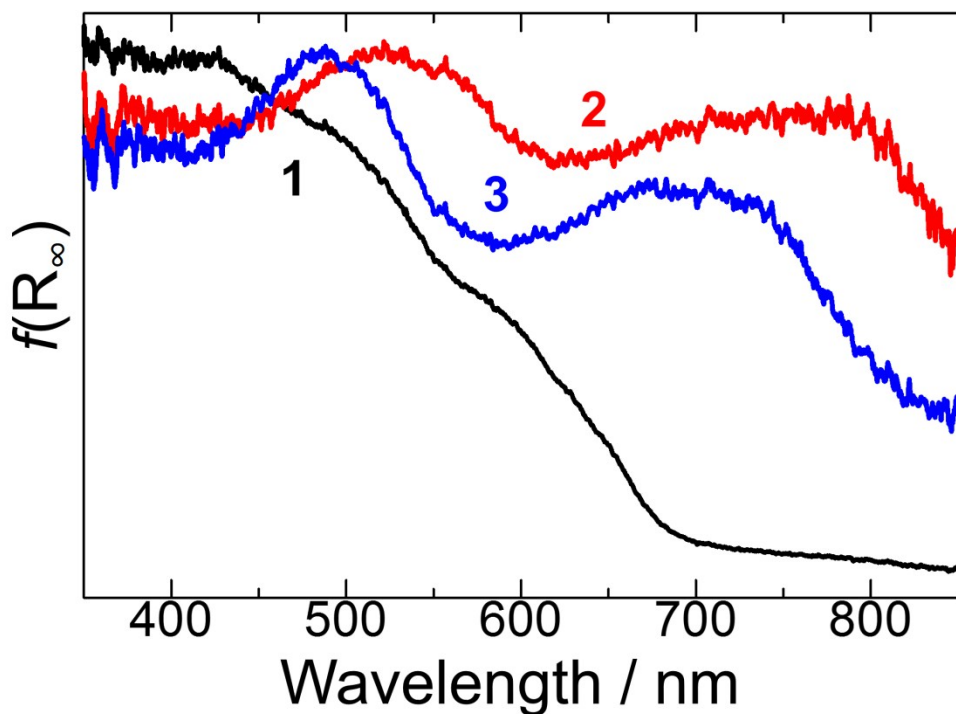
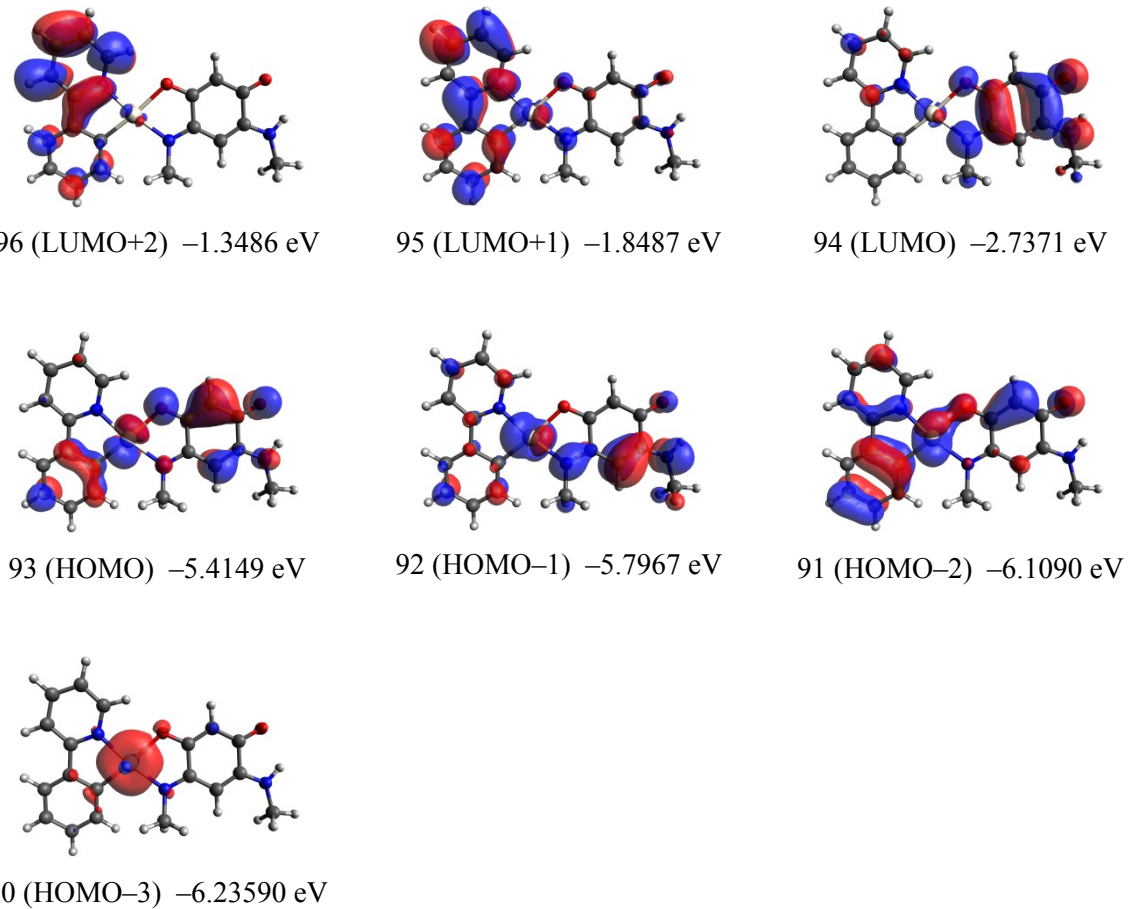


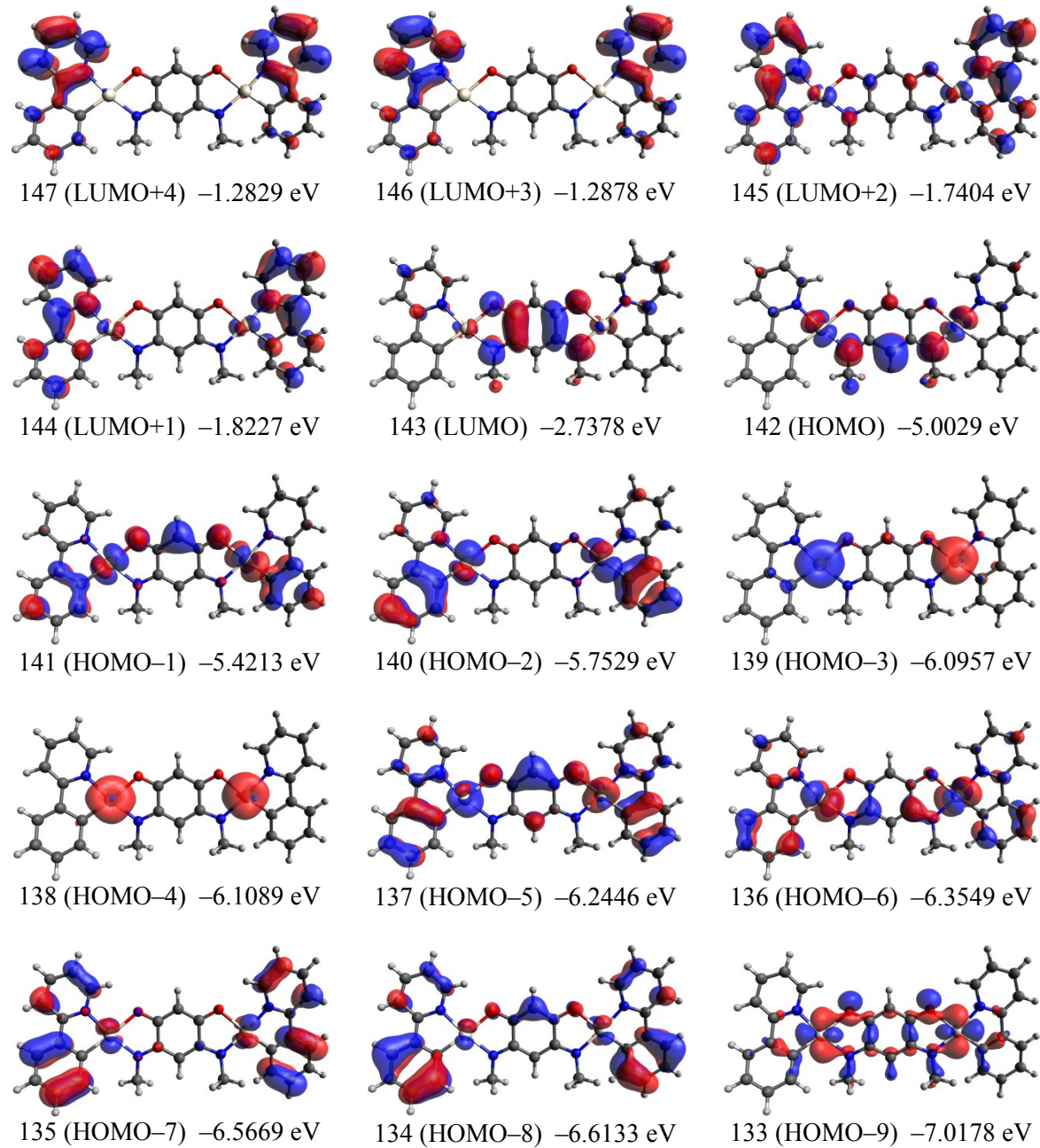
Fig. S6. UV–vis diffuse reflectance spectra for compounds **1** (black line), **2** (red line), and **3** (blue line) at room temperature. Observed absorption bands were almost similar to those of UV-vis absorption spectra in CH_2Cl_2 (Fig. 5), indicating that all three compound have only the weak or negligible intermolecular interactions in solid states, as suggested by X-ray crystallographic analyses (Fig. 1-3).

(a)



(continued)

(b)



(continued)

(c)

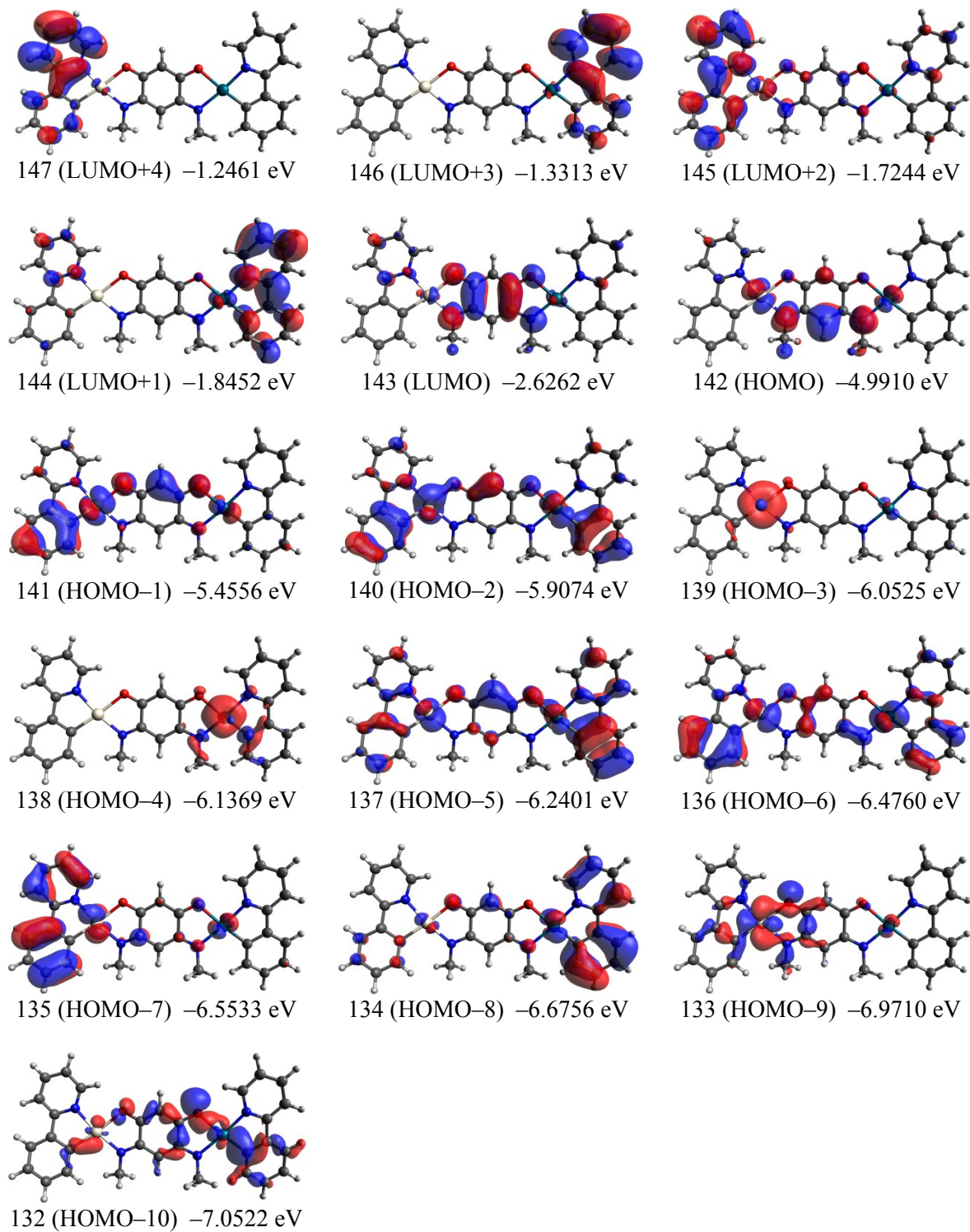
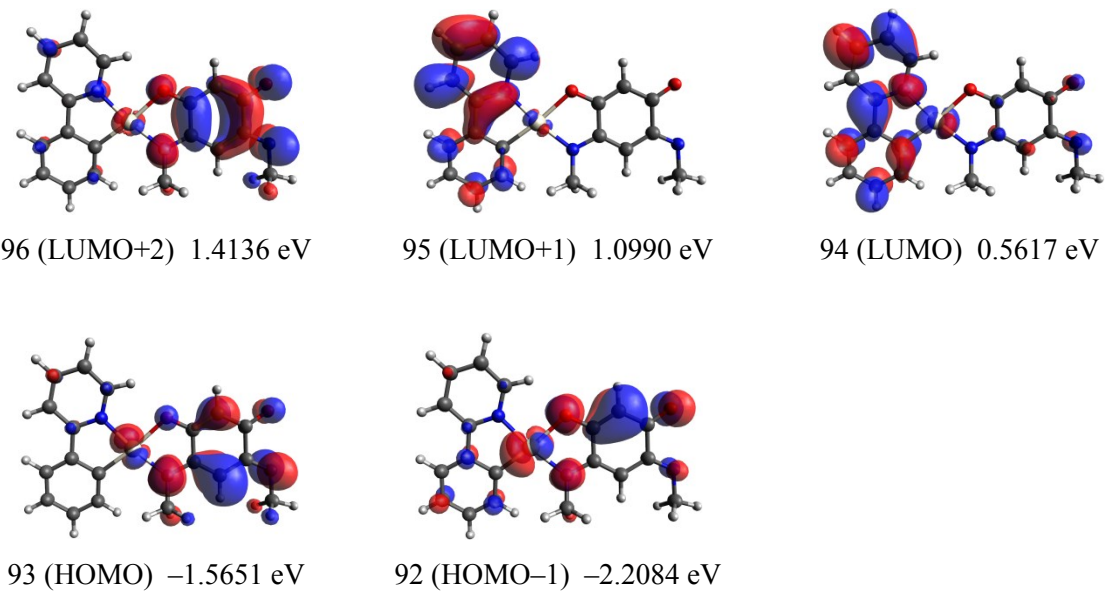


Fig. S7. Relevant calculated frontier orbitals for the electronic transitions observed in (a) **1**, (b) **2** and (c) **3**

(a)



(b)

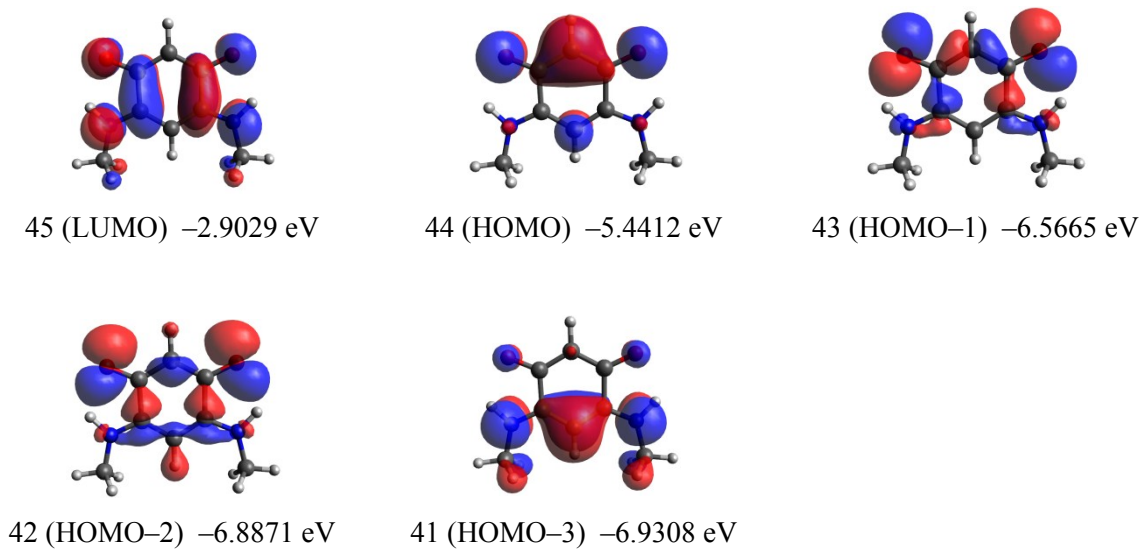


Fig. S8. Frontier orbitals of (a) $[1\text{-H}]^-$ (= deprotonated form of **1**, which was used as a synthetic intermediate of **2** and **3**) and (b) QH_2 .

Table S1. Bond distances within the [O,N,N,O] donor quinonoid moieties of complexes **1**, **2** and **3**:

Bond distances (Å)	1	2	3
C(12)-C(13)	1.53(1)	1.51(1)	1.49(1)
C(15)-C(16)	1.55(1)	1.52(1)	1.52(1)
C(13)-C(14)	1.43(1)	1.38(1)	1.41(1)
C(14)-C(15)	1.34(1)	1.39(1)	1.36(1)
C(12)-C(17)	1.35(1)	1.40(1)	1.39(1)
C(16)-C(17)	1.38(1)	1.39(1)	1.39(1)

Table S2. Electronic Spectra of the complexes in CH₂Cl₂.

Complex	$\lambda_{\text{max}}/\text{nm} (\epsilon / \text{M}^{-1}\text{cm}^{-1})$
1	551 (258.55), 444 (24089), 348 (16451)
2	740 (4774), 686 (4374), 512 (20137), 376 (7347)
3	701 (6209), 656 (6080), 478 (30668), 366 (13340)

Table S3. The electronic transitions of **1** calculated by the TD-DFT method, based on the optimized structure (The corresponding molecular orbitals are shown in Fig. S7).

Excited State	E (eV)	λ (nm)	f^{a} (> 0.01) ^b	Major contributions	$ \text{CI coef} (> 0.3)$
1	2.0552	603.28	0.0079	HOMO → LUMO	0.64782
2	2.6799	462.65	0.0351	HOMO-3 → LUMO	0.45633
				HOMO-2 → LUMO	0.45553
3	2.6888	461.12	0.1031	HOMO-3 → LUMO	0.49554
				HOMO-1 → LUMO	0.38173
5	2.9044	426.88	0.0596	HOMO → LUMO+1	0.61592
6	2.9300	423.16	0.3646	HOMO-2 → LUMO	0.34084
				HOMO-1 → LUMO	0.38739
11	3.5370	350.53	0.0514	HOMO-1 → LUMO+1	0.42204
				HOMO → LUMO+2	0.45458

^a Oscillator strength. ^b Except for the excited state 1.

Table S4. The electronic transitions of **2** calculated by the TD-DFT method, based on the optimized structure (The corresponding molecular orbitals are shown in Fig. S7).

Excited State	E (eV)	λ (nm)	f^a (> 0.01)	Major contributions	$ CI\ coef $ (> 0.3)
1	1.7796	696.68	0.0826	HOMO → LUMO	0.57602
2	2.3211	534.16	0.7620	HOMO-1 → LUMO	0.59004
7	2.7950	443.59	0.0316	HOMO → LUMO+2	0.64667
8	2.9580	419.15	0.1963	HOMO-5 → LUMO	0.62525
9	3.0327	408.83	0.0238	HOMO-1 → LUMO+1	0.58379
11	3.1010	399.82	0.0203	HOMO-2 → LUMO+1	0.31533
				HOMO-1 → LUMO+2	0.49864
12	3.2809	377.90	0.0249	HOMO → LUMO+3	0.66064
13	3.2917	376.66	0.0133	HOMO → LUMO+4	0.63706
14	3.3649	368.46	0.0181	HOMO-9 → LUMO	0.33107
				HOMO-7 → LUMO	0.48406
17	3.4086	363.74	0.0159	HOMO-8 → LUMO	0.55708

^a Oscillator strength.

Table S5. The electronic transitions of **3** calculated by the TD-DFT method, based on the optimized structure (The corresponding molecular orbitals are shown in Fig. S7).

Excited State	E (eV)	λ (nm)	f^a (> 0.01)	Major contributions	$ CI\ coef $ (> 0.3)
1	1.8728	662.03	0.0820	HOMO → LUMO	0.59004
2	2.4282	510.61	0.5123	HOMO-1 → LUMO	0.58332
3	2.6520	467.51	0.0403	HOMO-3 → LUMO	0.58126
4	2.6979	459.56	0.1563	HOMO-3 → LUMO	0.35863
				HOMO-2 → LUMO	0.41426
6	2.7632	448.69	0.0709	HOMO-4 → LUMO	0.57932
8	3.0629	404.79	0.0577	HOMO-5 → LUMO	0.48472
				HOMO-1 → LUMO+2	0.38380
9	3.0988	400.10	0.0674	HOMO-5 → LUMO	0.44002
				HOMO-1 → LUMO+1	0.32391
12	3.2919	376.64	0.0612	HOMO → LUMO+4	0.57761
14	3.3333	371.96	0.0265	HOMO-6 → LUMO	0.50978
				HOMO → LUMO+4	0.30332
17	3.4415	360.27	0.0144	HOMO-9 → LUMO	0.40376
				HOMO-7 → LUMO	0.45490
18	3.4662	357.70	0.0148	HOMO-10 → LUMO	0.48405

^a Oscillator strength.